Tech Science Press

Single-Layer Wideband Circularly Polarized Antenna Using Non-Uniform Metasurface for C-band Applications

Huy Hung Tran[1,2], Khoa Nguyen-Dang[1,2,*] and Niamat Hussain[3]

[1]Faculty of Electrical and Electronic Engineering, PHENIKAA University, Hanoi, 12116, Vietnam
[2]PHENIKAA Research and Technology Institute (PRATI), A&A Green Phoenix Group JSC,
Cau Giay, 11313, Hanoi, Vietnam
[3]Department of Computer and Communication Engineering,
Chungbuk National University, Cheongju 28644, Korea
*Corresponding Author: Khoa Nguyen-Dang. Email: khoa.nguyendang@phenikaa-uni.edu.vn
Received: 19 December 2020; Accepted: 29 January 2021

Abstract: A single-layer design of non-uniform metasurface (MS) based circularly polarized (CP) antenna with wideband operation characteristic is proposed and investigated in this paper. The antenna is excited by a truncated corner squared patch as a primary radiating CP source. Then, a non-uniform MS is placed in the same layer with the driven patch. Besides increasing the impedance bandwidth, the non-uniform MS also generates two additional CP bands in the high frequency band, leading to significantly increase the antenna's overall performances. The use of non-uniform MS distinguishes our design from the other CP MS based antennas in literature, in which the MS is formed by multiple uniform unit cells and placed in different layer with the radiating element. For validation, an antenna prototype, whose overall dimensions of $0.94\,\lambda_o \times 0.94\,\lambda_o \times 0.06\,\lambda_o$ at the center operating frequency, is fabricated and experimentally tested. The measured operating bandwidth with $|S_{11}| \leq -10\,dB$ and $AR \leq 3\,dB$ is $27.1\%\,(5.1-6.7\,GHz)$ and the broadside gain within this band is from 5.7 to 7.2 dBic. Compared to the other related works, the proposed antenna has advantage of very wideband operation with single-layer design.

Keywords: Circular polarization; metasurface; non-uniform; patch antenna; wideband

1 Introduction

The use of circularly polarized (CP) antenna has been illustrated as a useful method for multi-path interferences reduction as well as polarization mismatch mitigation. The antennas with simple design, low profile as well as wideband operation characteristics have received lots of attention from researchers. Single-fed patch antennas are considered as a potential candidate to satisfy the abovementioned requirements. However, an inherently narrow operating bandwidth (BW) caused by the high quality factor is a critical drawback of this antenna type [1]. Up to now, the task for BW enhancement of the single-fed CP patch antenna while maintaining low profile feature is still

very challenging. The most common method is to employ a low permittivity substrate, which is constructed with an air gap between a ground plane and a radiating element [2–9]. This method can significantly increase the BW up to approximately 24% [9]. However, the antenna's profile is typically higher than 0.1 λ_o (λ_o is the free-space wavelength at the center frequency). Alternatively, wideband performance is also attained by using a meandering probe fed technique [10,11]. Nonetheless, multiple stacked substrates are required in such designs, leading to high profile configuration. In recent years, metasurface (MS) have been widely applied to obtain the BW enhancement for microstrip patch or slot antennas while keeping low-profile structure [12–19]. The MS layer is generally formed by multiple periodical unit cells with various shapes, such as square, rectangular, H-shape, etc. Then, it is arranged above or below the radiating element. In general, this antenna type exhibits wide operation BW, which is typically less than 25%, and low-profile configuration of less than 0.1 λ_o. However, all of the abovementioned designs require for multiple printed layers. This makes the antenna more complicated and multi-layer design also causes some difficulties in fabrication. There are few single-layer antennas with wideband CP operation [20–22], but with limited BW of less than 20%.

In this paper, a low-profile MS based CP antenna with single layer and wideband operation characteristics is proposed for the C-band applications (4–8 GHz) [23]. It is noted that unlike the conventional CP MS antennas [12–19], where the MS is comprised of multiple uniform unit cells and positioned in different layer with the radiating source, this paper takes a different approach. Here, the MS is formed by non-uniform unit cells and designed in the same layer with the driven patch. The proposed MS is able to generate additional resonances, which are then combined with the original one from the driven patch to achieve wide operating BW. The proposed design is an extension of the work in [20], but with significant BW enhancement of about 40%. Besides, the use of non-uniform MS to improve the performance of CP antenna has not been presented in literature. These are the main contributions of our paper. The proposed design is first character-ized in full-wave simulation tool High-Frequency Structure Simulator (HFSS) and then validated by measurements.

2 Principle for Operation

To have wideband operation, the driven patch and the MS are designed so that their operating bands are closed to each other. The square patch with corner truncation will work at the lowest band. Its dimension (W_p) for operation at the fundamental TM_{11} mode (f_r) can be approximately defined by:

$$W_p = \frac{c}{2f_r\sqrt{\varepsilon_{eff}}} \sim \frac{c}{2f_r\sqrt{\frac{\varepsilon_r+1}{2}}} \tag{1}$$

where c is the speed of light, ϵ_{eff} is the effective permittivity of the substrate. Next, the MS is designed to have operation in higher frequency band. The resonance of the surface waves, which propagate on the finite-sized MS, can be qualitatively calculated by [12,24]:

$$\beta_{sw} = \frac{m\pi}{N \times P}; \quad m = 1, 2, \ldots \tag{2}$$

where, β_{sw} is the propagation constant, N and P is respectively the unit cell number and the cell's periodicity. In this paper, the MS is formed by non-uniform metallic plates but with similar peri-odicity. Fig. 1 presents the dispersion diagram of different unit cells at the first two eigenmodes (transverse magnetic-TM and transverse electric-TE). As seen, the size of the metallic plate (W_o)

has great impact on the operating behavior of the TM and TE modes. By properly choosing the value of m and N, multiple adjacent resonances can be achieved. For Case-1 with $m = 2$, the MS with 4×4 cells configuration is expected to work at 6.5 and 6.8 GHz. For Case-2 with $m = 3$, the 6×6 MS will have operation around 7.7 and 8.9 GHz.
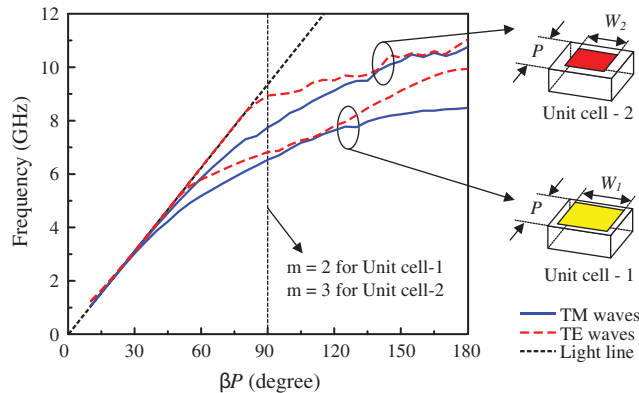

Figure 1: Dispersion diagram of different unit cells. The parameters are as follows: $P = 8$ mm, $W_1 = 7.5$ mm, $W_2 = 5$ mm

3 Antenna Design

3.1 Antenna with Uniform Metasurface

The geometrical configuration of the wideband CP antenna with uniform MS is illustrated in Fig. 2. The antenna is constructed with a driven microstrip patch, a MS and a ground plane. The antenna is fabricated on a single layer of a Taconic RF-35 substrate (permittivity of $\epsilon_r = 3.5$ and loss tangent of $tan\delta = 0.0018$). The driven patch with truncated corners acting as a primary radiating CP source of the proposed design is located at the center and surrounded by multiple MS unit cells. The antenna is fed by the 50 Ω SMA connector. The optimized design dimensions of this antenna are as follows: $W_s = 32$, $H_s = 3$, $W_p = 13.3$, $d = 5$, $L_f = 13.5$, $W_f = 3$, $P = 8$, $W_1 = 7.5$, $g = 0.3$ (unit: mm).
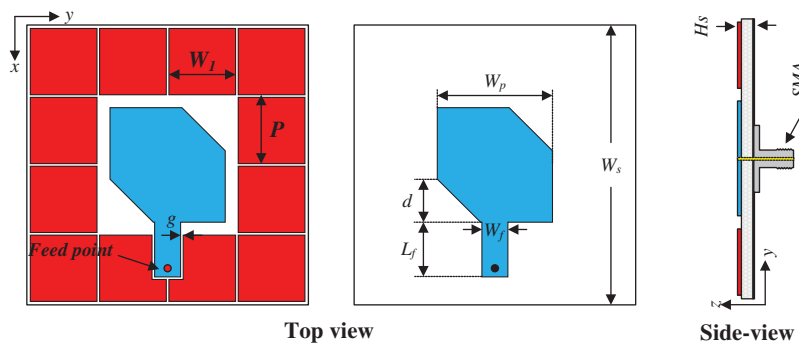

Figure 2: Geometry of the single-layer CP antenna with uniform MS

The previous studies [12–19] design the MS on a different layer from the driven element, which increases the design complexity and cost. In this paper, all of the radiating components are printed in the same layer. The evolution to achieve the final design is presented in Fig. 3. In the first stage, antenna without MS as Antenna-1 is considered. Then, the patch is embedded into the center of the 4×4 unit cells MS as Antenna-2 and finally, Antenna-3 is obtained by removing four center unit cells. The performance comparison of these antennas is presented in Fig. 4. The simulated data indicates that Antenna-1 has narrow band operation. When MS is introduced, additional bands in the high frequency region are observed in both $|S_{11}|$ and AR profiles. Finally, Antenna-3 shows significant enhancement in the operating BW of 21% (5.12–6.32 GHz). It is noted that, besides the lower resonances at 5.2 and 5.6 GHz in the $|S_{11}|$ profile produced by the driven patch, there also exist two additional resonances at 6.1 and 6.6 GHz. These resonances are generated by the MS and they are quite matched with the prediction band on the dispersion diagram in Fig. 1. In terms of AR, there are two CP bands around 5.3 and 6.1 GHz, which are respectively produced by the driven patch and the MS. For better demonstration, Fig. 5 presents the simulated results of $|S_{11}|$ and AR for different sizes of the patch (W_p) and the unit cell (W_1). It can be seen that tuning W_p has strong impact on the lower $|S_{11}|$ resonances and the first CP band, which shift upwards as decreasing W_p. Meanwhile, the higher $|S_{11}|$ resonances and the CP band are almost stable with the variation of W_p. Similar behavior for higher band operation when tuning W_1 can be observed in Fig. 5b. Two highest $|S_{11}|$ resonances and the second CP band move towards higher frequency range as decreasing W_1. The data confirms that the patch is critical for the lower band operation, while higher range is produced by the MS.
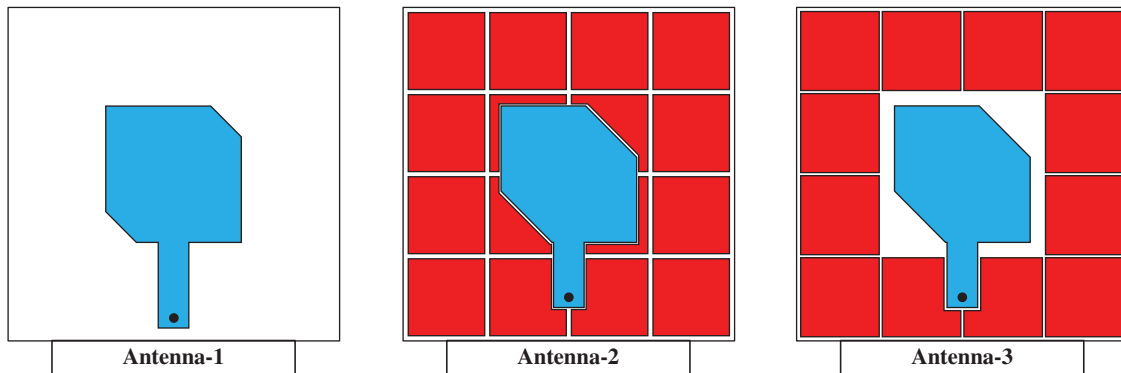

Figure 3: Design evolution of the final design

3.2 Antenna with Non-Uniform Metasurface

Based on the abovementioned design, additional array of MS is inserted as Antenna-4 depicted in Fig. 6. Similar to the previous MS, all the center unit cells of the additional 6×6 MS are removed. The optimized design dimensions of Antenna-4 are as follows: $W_s = 48$, $H_s = 3$, $W_p = 13.3$, $d = 5$, $L_f = 16$, $W_f = 2.6$, $P = 8$, $W_1 = 7.5$, $W_2 = 5$, $g = 0.5$ (unit: mm).
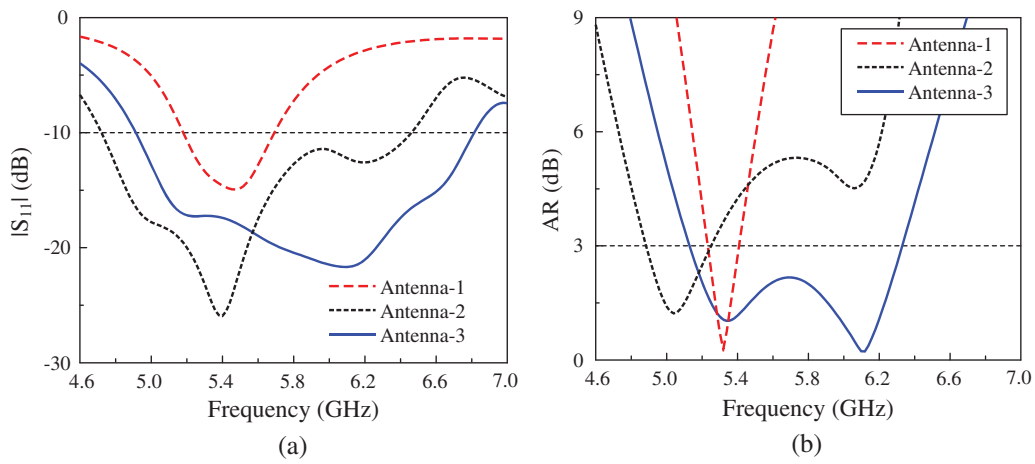
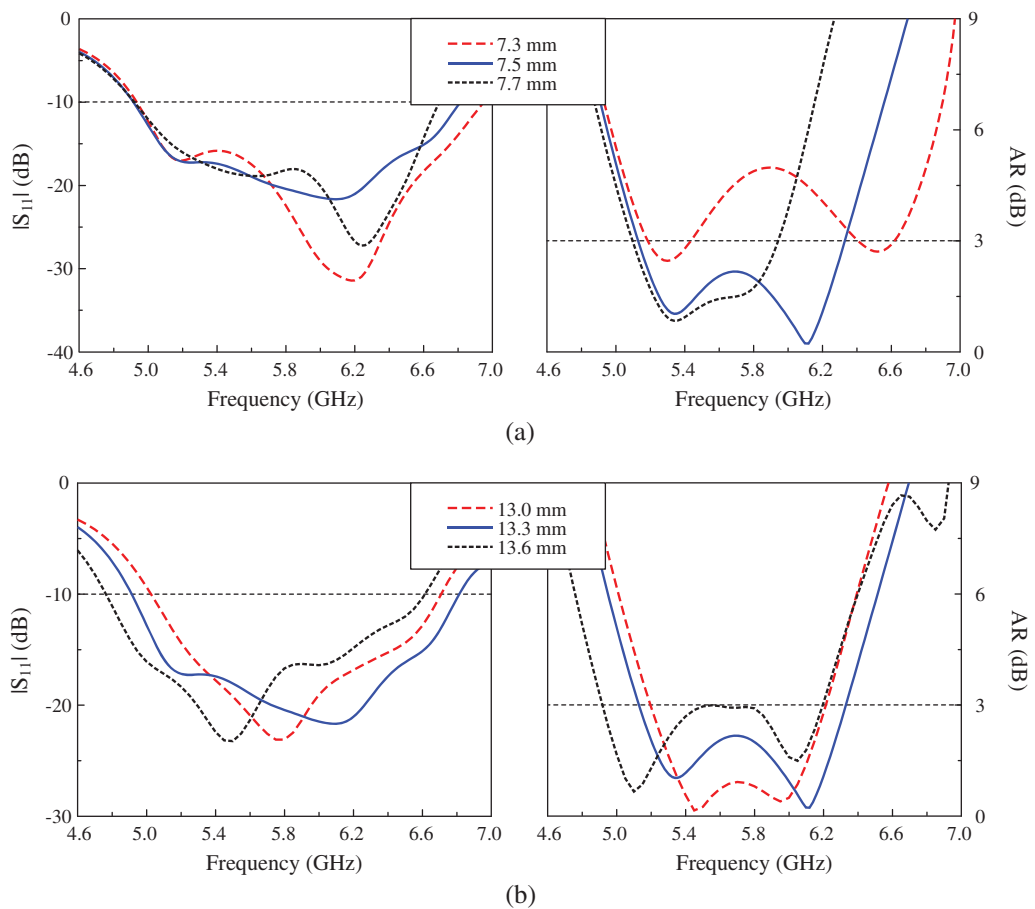**Figure 4:** Simulated performances of different antenna configurations. (a) |S$_{11}$|, (b) AR

Figure 5: Simulated |S$_{11}$| and AR of Antenna-3 for different values of (a) W_1 and (b) W_p
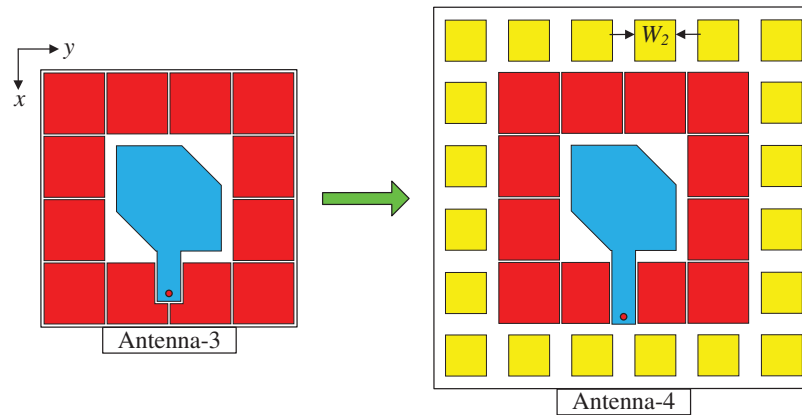
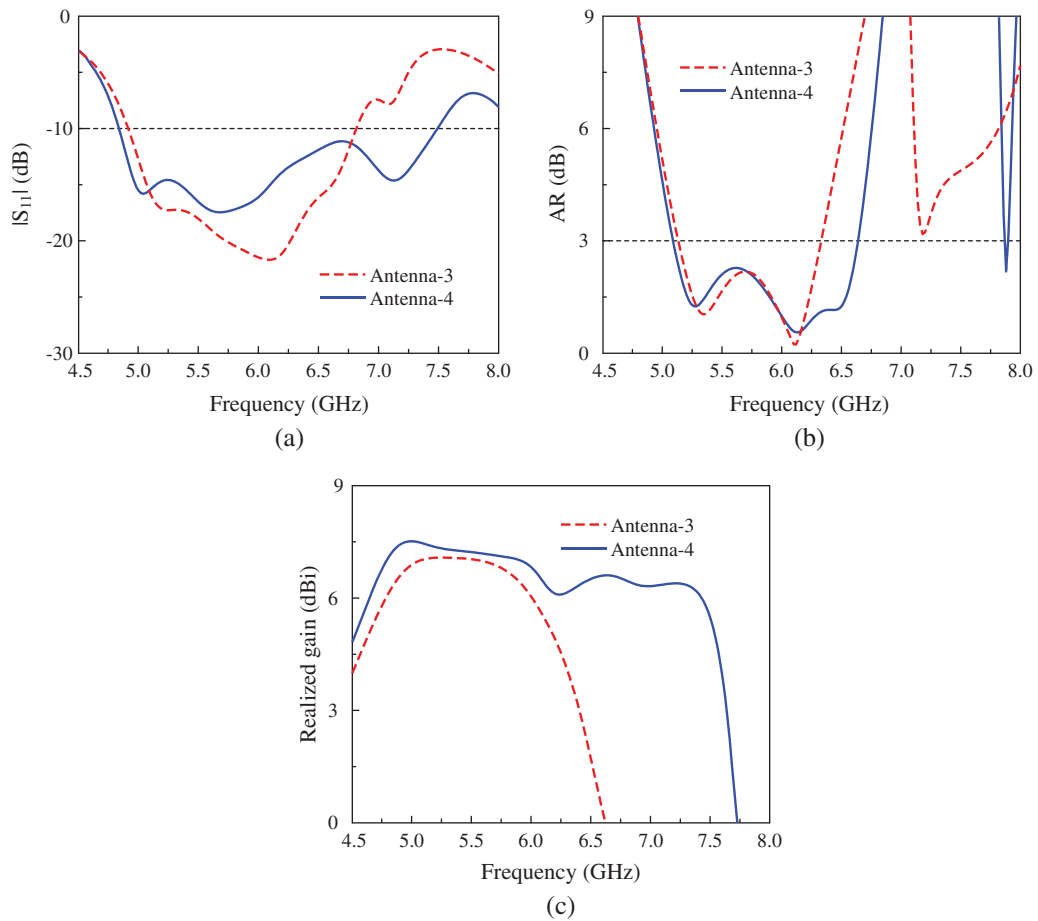**Figure 6:** Geometry of the antenna with non-uniform MS

Figure 7: Simulated (a) $|S_{11}|$, (b) AR, and (c) gain of the antenna with uniform MS and non-uniform MS

The simulated performances of the antenna with uniform MS and non-uniform MS are illustrated in Fig. 7. It can be seen that by using non-uniform MS, an additional $|S_{11}|$ resonance at 7.1 GHz is generated for Antenna-4. Thus, the impedance BW of the antenna increases from 32.4% (4.92–6.82 GHz) to 42.9% (4.84–7.48 GHz). Besides, another CP band at 6.5 GHz is also realized and the overall 3 dB AR BW improves from 21% (5.12–6.32 GHz) to 26.6% (5.08–6.64 GHz). In fact, the additional $|S_{11}|$ and CP bands can be adjusted by tuning the size of the outer MS unit cell, W_2. Fig. 8 shows the $|S_{11}|$ and AR for different values of W_2. Obviously, tuning W_2 only has significant influence on the highest $|S_{11}|$ and CP bands, which increase as W_2 decreases. Meanwhile, the lower operating bands are almost stable with the variation of W_2. In terms of broadside gain, Antenna-3 observes a significant drop in the high frequency region of greater than 6.2 GHz. For Antenna-4 with additional MS, the gain is increased in higher band and the gain is better than 6 dBi over very wide frequency range from 4.6 to 7.4 GHz.
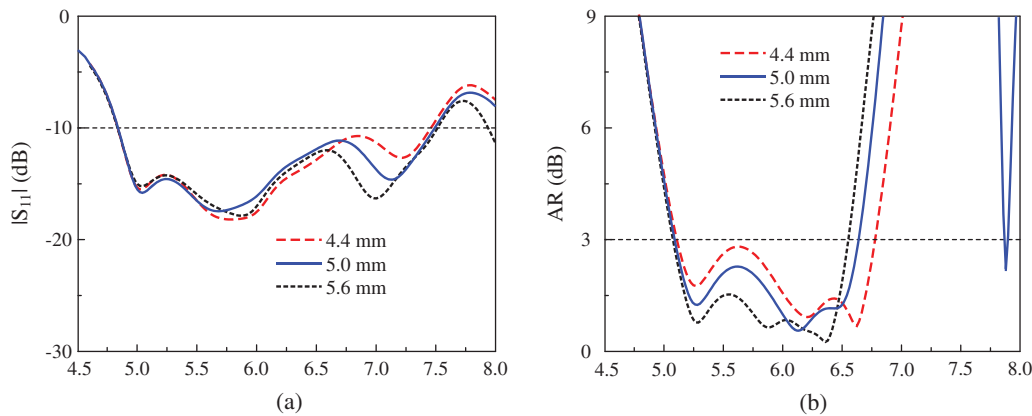

Figure 8: Simulated (a) $|S_{11}|$ and (b) AR of Antenna-4 with different values of W_2

In order to optimize this antenna, the feeding line is very important parameter to the matching performance, which is demonstrated in Fig. 9. The simulated data indicates that increasing L_f results in better impedance matching. However, when L_f is larger than 18 mm, the matching is degraded.
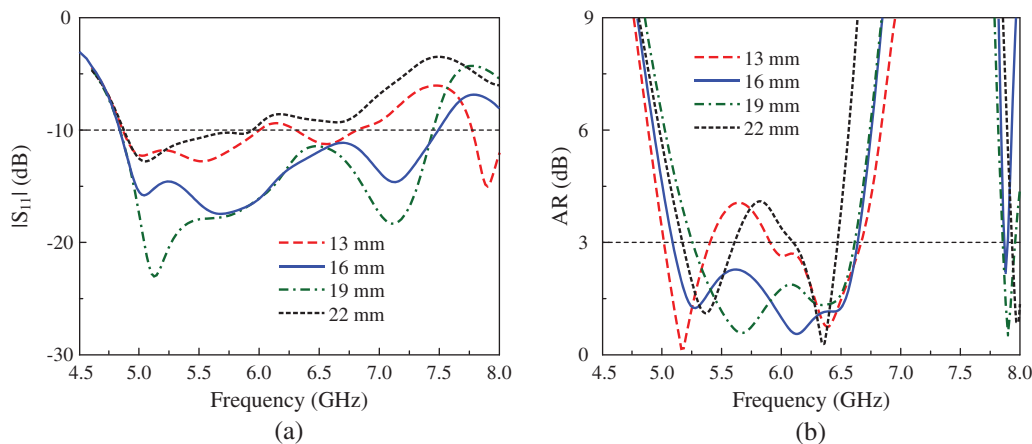

Figure 9: Simulated (a) $|S_{11}|$ and (b) AR results of Antenna-4 with different values of L_f

4 Measurement Results

The proposed wideband CP antenna using non-uniform MS was fabricated using etching technique as shown in Fig. 10. The antenna's reflection coefficient was measured using the PNA Network Analyzer N5224A and the far-field characteristics were implemented in an anechoic chamber by Microwave Technologies Group [25]. The chamber is fully installed with electrically-thick foam absorber and two horn antennas are employed as reference antennas. The testing antenna is mounted on a computer-controlled rotating positioner. Generally, the measured data is well matched with the simulated one. It still exists several discrepancies due to the tolerance in fabrication and imperfection in measurement setup.

Figure 10: Photograph of fabricated antenna

The simulated and tested $|S_{11}|$ results of the proposed antenna are presented in Fig. 11a. The antenna shows good impedance matching in a wide frequency band from 4.9 to 7.4 GHz, equivalent to 40.7%. Fig. 11b depicts the far-field radiation characteristics in terms of AR and realized gain in broadside direction. As observed, the measured 3 dB AR BW is 27.1%, ranging from 5.1 to 6.7 GHz, and along with this, the measured gain is from 5.7 to 7.2 dBic. Fig. 12 plots the antenna gain radiation patterns in two principal (x-z and y-z planes) at different operating frequencies. As observed, the right-hand CP (RHCP) is the dominant r mode over the left-hand CP (LHCP). At the broadside direction ($\theta = 0°$), the polarization isolation defined by the difference gain levels of the RHCP and LHCP is higher than 16 dB. Besides, the front-to-back ratio is always greater than 15 dB in the whole band.
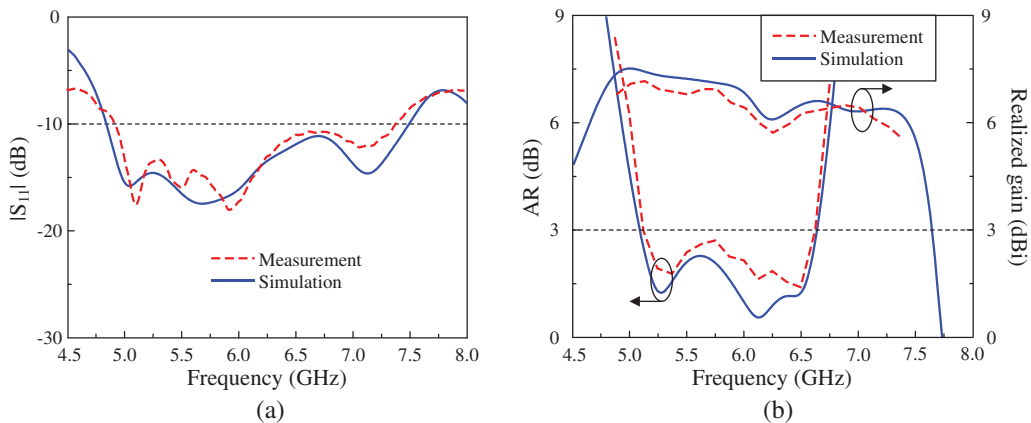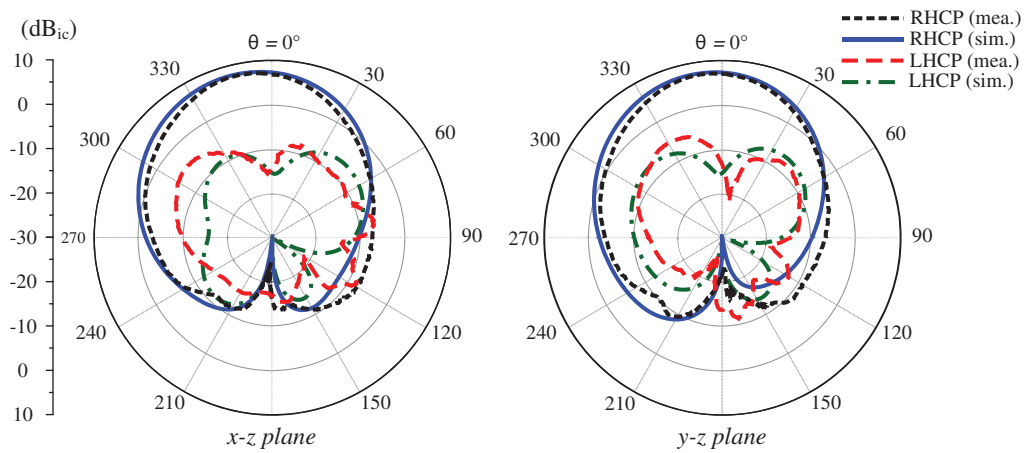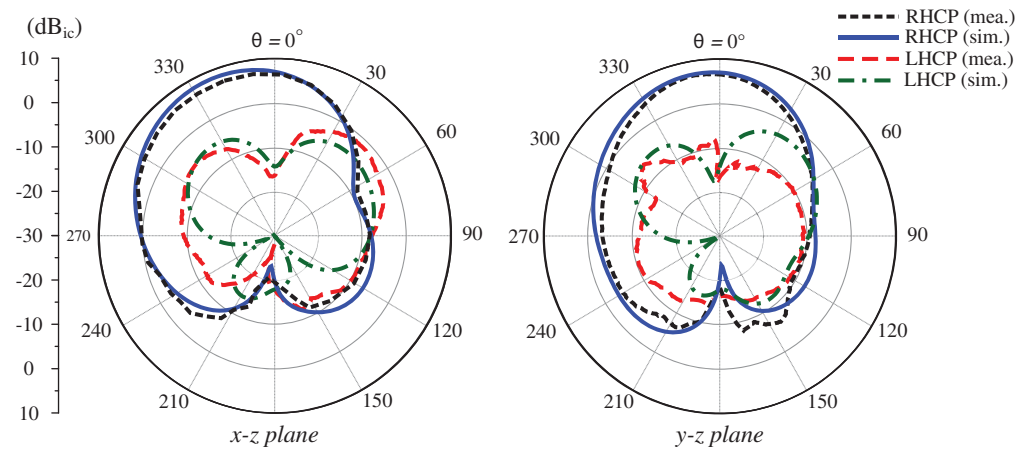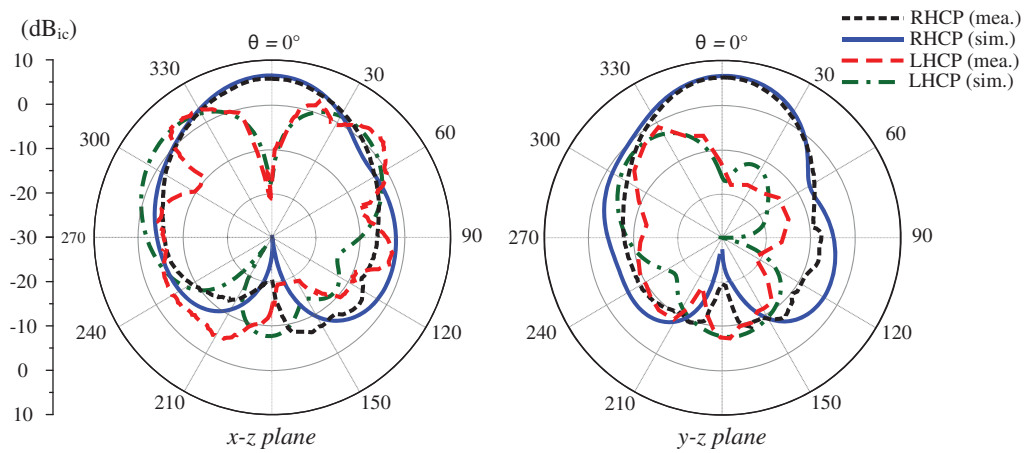

Figure 11: Simulated and measured (a) $|S_{11}|$ and (b) AR and gain of the proposed antenna

Figure 12: Simulated and measured gain radiation patterns of the proposed antenna. (a) 5.3 GHz, (b) 5.9 GHz, (c) 6.5 GHz

The performance comparison among the low-profile, wideband CP antennas is tabulated in Tab. 1. As seen, the presented antenna shows the best operating BW among the single-layer designs [20–22]. Besides, the presented work has wider BW than most of other multi-layer ones. Although the designs in [14,15] have wider operating BW, their structures are more complicated than that of the proposed design.

Table 1: Performance comparison among the low-profile, single-fed, wideband CP antennas

Antennas	Overall size (λ_o)	Single-layer design	CP BW (%)	Gain (dBic)
Ref. [2]	$1.04 \times 1.04 \times 0.13$	No	17.1	9.5
Ref. [5]	$0.80 \times 0.80 \times 0.09$	No	17.9	8.7
Ref. [6]	$1.07 \times 0.87 \times 0.11$	No	18.0	7.5
Ref. [8]	$0.81 \times 0.81 \times 0.09$	No	20.3	8.6
Ref. [9]	$1.14 \times 1.14 \times 0.13$	No	23.9	8.5
Ref. [10]	$0.63 \times 0.63 \times 0.14$	No	16.9	7.4
Ref. [12]	$0.58 \times 0.58 \times 0.06$	No	23.4	7.6
Ref. [13]	$0.78 \times 0.80 \times 0.10$	No	20.4	6.5
Ref. [14]	$0.85 \times 0.85 \times 0.05$	No	31.3	7.0
Ref. [15]	$1.18 \times 0.97 \times 0.07$	No	28.9	6.8
Ref. [19]	$0.53 \times 0.53 \times 0.05$	No	26.2	6.7
Ref. [20]	$0.60 \times 0.60 \times 0.06$	Yes	19.7	6.9
Ref. [21]	$0.32 \times 0.32 \times 0.01$	Yes	15.8	N/G
Ref. [22]	$0.86 \times 0.86 \times 0.04$	Yes	12.8	8.4
Proposed	$0.94 \times 0.94 \times 0.06$	**Yes**	**27.1**	**7.2**

5 Conclusion

A single-layer MS based wideband CP antenna has been presented and investigated in this paper. This paper utilizes a non-nuniform MS, which has potential to not only increase the impedance BW but also produce two additional CP bands to significantly widen the overall 3-dB AR BW of the proposed design. The measurements implemented on a fabricated antenna demonstrate that wide operating BW of 27.1% (5.1–6.7 GHz) is attained. Additionally, the antenna also exhibits good radiation characteristics and gain in broadside direction of better than 5.7 dBic. The proposed antenna can be a potential candidate for communication systems in C-band, such as wireless local area network (WLAN), satellite, cordless telephones and so on.

Conflicts of Interest: The authors declare that they have no conflicts of interest to report regarding the present study.

References

[1] P. C. Sharma and K. C. Gupta, "Analysis and optimized design of single feed circularly polarized microstrip antennas," *IEEE Transactions on Antennas and Propagation*, vol. 31, no. 6, pp. 949–955, 1983.
[2] J. Wu, W. Hu, Y. Yin and R. Lian, "Broadband circularly polarized antennas with center-slot-feeding," *Microwave and Optical Technology Letters*, vol. 57, no. 12, pp. 2793–2797, 2015.

[3]   N. Hussain, M. Jeong, J. Park and N. Kim, "A broadband circularly polarized Fabry-Perot resonant antenna using a single-layered PRS for 5G MIMO applications," *IEEE Access*, vol. 7, pp. 42897–42907, 2019.

[4]   D. A. Sehrai, F. Muhammad, S. H. Kiani, Z. H. Abbas, M. Tufail *et al.,* "Gain-enhanced metamaterial based antenna for 5G communication standards," *Computers, Materials & Continua*, vol. 64, no. 3, pp. 1587–1599, 2020.

[5]   J. Wu, X. Ren, Z. Wang and Y. Yin, "Broadband circularly polarized antenna with L-shaped strip feeding and shorting-pin loading," *IEEE Antennas and Wireless Propagation Letters*, vol. 13, pp. 1733–1736, 2014.

[6]   T. Mondal, S. Maity, R. Ghatak and S. R. B. Chaudhuri, "Design and analysis of a wideband circularly polarized perturbed psi-shaped antenna," *IET Microwaves, Antennas & Propagation*, vol. 12, no. 9, pp. 1582–1586, 2018.

[7]   J. Li, H. Liu, S. Zhang, M. Luo, Y. Zhang *et al.,* "A wideband single-fed, circularly-polarized patch antenna with enhanced axial ratio bandwidth for UHF RFID reader applications," *IEEE Access*, vol. 6, pp. 55883–55892, 2018.

[8]   W. Yang, J. Zhou, Z. Yu and L. Li, "Single-fed low profile broadband circularly polarized stacked patch antenna," *IEEE Transactions on Antennas and Propagation*, vol. 62, no. 10, pp. 5406–5410, 2014.

[9]   J. Wu, Y. Yin, Z. Wang and R. Lian, "Broadband circularly polarized patch antenna with parasitic strips," *IEEE Antennas and Wireless Propagation Letters*, vol. 14, pp. 559–562, 2015.

[10] Q. W. Lin, H. Wong, X. Y. Zhang and H. W. Lai, "Printed meandering probe-fed circularly polarized patch antenna with wide bandwidth," *IEEE Antennas and Wireless Propagation Letters*, vol. 13, pp. 654–657, 2014.

[11] H. Wong, Q. W. Lin, H. W. Lai and X. Y. Zhang, "Substrate integrated meandering probe-fed patch antennas for wideband wireless devices," *IEEE Transactions on Components, Packaging and Manufacturing Technology*, vol. 5, no. 3, pp. 381–388, 2015.

[12] S. X. Ta and I. Park, "Low-profile broadband circularly polarized patch antenna using metasurface," *IEEE Transactions on Antennas and Propagation*, vol. 63, no. 12, pp. 5929–2934, 2015.

[13] T. Nakamura and T. Fukusako, "Broadband design of circularly polarized microstrip patch antenna using artificial ground structure with rectangular unit cells," *IEEE Transactions on Antennas and Propagation*, vol. 59, no. 6, pp. 2103–2110, 2011.

[14] S. Liu, D. Yang and J. Pan, "Wideband circularly polarized patch antennas on reactive impedance substrates," *IEEE Antennas and Wireless Propagation Letters*, vol. 18, no. 7, pp. 1395–1399, 2019.

[15] S. S. Jash, C. Goswami and R. Ghatak, "A low profile broadband circularly polarized planar antenna with an embedded slot realized on a reactive impedance surface," *AEU-International Journal of Electronics and Communications*, vol. 108, no. 1, pp. 62–72, 2019.

[16] C. Zhao and C. F. Wang, "Characteristic mode design of wide band circularly polarized patch antenna consisting of H-shaped unit cells," *IEEE Access*, vol. 6, pp. 25292–25299, 2018.

[17] S. Liu, D. Yang and J. Pan, "A low-profile circularly polarized metasurface antenna with wide axial-ratio beamwidth," *IEEE Antennas and Wireless Propagation Letters*, vol. 18, no. 7, pp. 1438–1442, 2019.

[18] Y. Juan, W. Yang and W. Che, "Miniaturized low-profile circularly polarized metasurface antenna using capacitive loading," *IEEE Transactions on Antennas and Propagation*, vol. 67, no. 5, pp. 3527–3532, 2019.

[19] Q. Chen and H. Zhang, "Dual-patch polarization conversion metasurface-based wideband circular polarization slot antenna," *IEEE Access*, vol. 6, pp. 74772–74777, 2018.

[20] H. H. Tran, N. Hussain and T. T. Le, "Single-layer low-profile wideband circularly polarized patch antenna surrounded by periodic metallic plates," *International Journal of RF and Microwave Computer-Aided Engineering*, vol. 29, no. 12, pp. e21969, 2019.

[21] Z. L. Yang, L. Zhu and S. Xiao, "An implantable wideband circularly polarized microstrip patch antenna via two pairs of degenerate modes," *IEEE Access*, vol. 7, pp. 4239–4247, 2019.

[22] Z. Liang, J. Ouyang and F. F.Yang, "Low-profile wideband circularly polarized single-layer metasurface antenna," *Electronics Letters*, vol. 54, no. 24, pp. 1362–1364, 2018.

[23] Accessed Dec. 28, 2020, [Online]. Available: https://en.wikipedia.org/wiki/C_band_(IEEE).

[24] F. Costa, O. Luukkonen, C. R. Simovski, A. Monorchio, S. A. Tretyakov *et al.,* "TE surface wave resonances on high-impedance surface based antennas: Analysis and modeling," *IEEE Transactions on Antennas and Propagation*, vol. 59, no. 10, pp. 3588–3596, 2011.

[25] Accessed May 15, 2020, [Online]. Available: http://www.mtginc.co.kr.